MLTJ
Muscles, Ligaments and Tendons Journal

ORIGINAL ARTICLE

THE EFFECT OF LOW-INTENSITY ELECTROACUPUNCTURE ON FIBROUS REPAIR IN CHRONIC ROTATOR CUFF INJURY INDUCED BY SUBACROMIAL IMPINGEMENT

Zelin Wu[1]*, Zihang Chen[1]*, Zhoucheng Wan[1]*, Chuangye Chen[2]*, Kuixiang Wang[3], Nan Ru[1], Siyuan Xie[1], Lili Zhao[3], Zhiqiang Jia[3], Kin Chiu[4], Yanping Gao[5], Xiaofei Zheng[1], Jian Guan[6], Huajun Wang[1]

[1] Department of Sports Medicine, The First Affiliated Hospital, Subingtian Center for Speed Research And Training/Guangdong Key Laboratory of Speed Capability Research, The Guangzhou Key Laboratory of Precision Orthopedics and Regenerative Medicine, School of Medicine, Jinan University, Guangzhou, China
[2] Guangdong Provincial Key Laboratory of Speed Capability Research, Jinan University Su Bingtian Center for Speed Research and Training, School of Physical Education, Jinan University, Guangzhou, China
[3] Department of Orthopedics and Joint Surgery, Xingtai People's Hospital, Xingtai, China
[4] Department of Psychology, State Key Laboratory of Brain and Cognitive Sciences, The University of Hong Kong, Hong Kong, China
[5] Department of Traditional Chinese Orthopedics and Traumatology, Center for Orthopedic Surgery, The Third Affiliated Hospital of Southern Medical University, Guangzhou, China
[6] Department of Orthopedics, the Third Hospital of Shijiazhuang, Shijiazhuang, China
* Contributed equally

Corresponding author's e-mail: 467999223@qq.com; whj323@126.com

Received: 07/06/2026
Accepted: 17/07/2026
Published: 17/09/2026

Conflict of interests: The Authors declare that there are no competing interests.
Fundings: This work was project supported by National Natural Science Foundation of China (82374558, 82074511, 81973660), the National Key Research and Development Program of China (2023YFC2414500), the Fundamental Research Funds for the Central Universities (21625116, 21625120, 21623119), Science and Technology Projects in Guangzhou (202102070001), Natural Science Foundation of Guangdong Province (2023A1515140034), Medical Key Specialty Construction Project of the 14th Five-Year Plan in Foshan.
Data availability: The datasets generated and analyzed during the current study are available from the corresponding author upon reasonable request.
Contributions: Z Wu, Z C, K W, C C, and Z Wan contributed equally as co-first authors. J G, Y G, H W and X Z participated in the conception and design of the study. Material preparation, data collection, and analysis were performed by N R, S X, L Z and K C. K W, C C, Z C and Z Wu were responsible for visualization and writing the original draft. J G, Y G, H W and X Z contributed to the review and editing of the manuscript. H W and X Z supervised the project and secured funding.
This article is licensed under a CC Attribution-NonCommercial-NoDerivatives 4.0 License

LEVEL OF EVIDENCE: 5

ABSTRACT

Background: Electroacupuncture (EA) has been applied for sports injury rehabilitation, while its efficacy and molecular mechanisms in chronic rotator cuff tendon repair remain unclear. This study aimed to explore the therapeutic effects and underlying mechanisms of low-intensity EA on fibrous repair in subacromial impingement-induced chronic rotator cuff injury.

Materials and methods: A mouse model of chronic rotator cuff injury was established and treated with low-intensity EA (2 Hz, 0.1A, 15 min/day) for 2 and 4 weeks. Behavioral, muscular, biomechanical and histological assessments, together with IHC, qPCR and Western blot analyses were performed for comprehensive evaluation.

Results: EA significantly improved motor function, gait stability and tendon histological structure by mitigating inflammation and promoting ordered collagen reconstruction. EA upregulated *Col1a1*, *Col2a1*, tendon maturation (*Scx*, *Tnmd*) and antioxidant genes (*Sod2*, *Gpx1*) and downregulated pro-inflammatory factors, *Mmp13*, *Pparγ* and *Fabp4*, with consistent protein expression changes. *Conclusion:* In our mouse model of rotator cuff injury induced by subacromial impingement, low-intensity electroacupuncture improved histology, biomechanics, inflammation, fatty infiltration markers, and tendon maturation markers. However, clinical translation will require additional controlled preclinical studies, including sham stimulation and longer follow up.

Publisher smc media srl

KEYWORDS
Acupuncture, chronic rotator cuff injury, electroacupuncture, electrical stimulation, shoulder pain, subacromial impingement

INTRODUCTION

Shoulder pain severely impairs daily life and occupational ability, placing enormous socioeconomic pressure on society. The annual cost of treating shoulder dysfunction reaches nearly 7 billion USD in the United States, constituting a heavy global healthcare economic burden[1]. As a leading cause of shoulder pain, subacromial impingement syndrome accounts for approximately 50% of clinical cases; subacromial bony spurs and coracoacromial ligament hypertrophy induce mechanical friction and subsequent shoulder pain[2,3].

Chronic rotator cuff injury is induced by age-related degeneration, metabolic disorders, acute or repetitive microtrauma and immune microcirculation dysfunction[4,5], and subacromial impingement is well recognized as a key factor driving the initiation and progression of chronic rotator cuff lesions[6,7].

Growing fitness participation and higher rehabilitation requirements for competitive sports have greatly increased clinical demands for sports injury intervention. Non-invasive physical therapy has become the core rehabilitation method for sports injuries with high safety and reliable functional recovery effects[8,9]. Electrical stimulation therapy, featured by precise positioning, has been widely applied in musculoskeletal rehabilitation and validated for good efficacy and safety, linking basic research and clinical rehabilitation practice[10]. Multiple clinical studies have confirmed its therapeutic value: combined electrical stimulation and exercise training achieves long-term stable improvement of chronic ankle instability[10]; postoperative electrical stimulation effectively accelerates early shoulder functional recovery within six weeks after rotator cuff arthroscopy, relieves pain and muscle atrophy, improves shoulder mobility and muscle strength, and reduces kinesiophobia, with therapeutic effects lasting up to three months[11,12]. Ultrasound-guided precise EA treatment significantly relieves symptoms and improves shoulder mobility in 85% of rotator cuff injury patients after two months of intervention, realizing effective conservative treatment[13]. Animal experiments further support the tendon repair function of EA: EA increases the number of reparative cells and β-FGF+ cells in injured tendons, enhances tendon maximum tensile strength, elevates collagen deposition, and optimizes collagen fiber arrangement to facilitate high-quality tendon repair[14-16].

This work constructed subacromial impingement-induced chronic rotator cuff injury mouse models with local EA intervention on injured sites. This research aimed to verify EA's therapeutic effect, supply reliable experimental evidence for its clinical transformation, and establish experimental support for follow-up molecular mechanistic exploration.

MATERIALS AND METHODS

Ethics permission

All animal experiments in this study have been reviewed and approved by the institutional ethics committee (Jinan University n. 20250222-13). Male C57BL/6 mice aged 8 weeks were housed in a specific pathogen-free facility with a 12-hour light/dark cycle, constant temperature (22 ± 2°C), and free access to standard rodent chow and sterile water. All invasive surgeries were performed under general anesthesia induced by an isoflurane vaporizer. Predefined humane endpoints, including severe weight loss, persistent immobility, self-mutilation and organ failure, were closely monitored to terminate animal suffering in a timely manner. At the experimental endpoint, mice were humanely euthanized via overdose anesthesia in accordance with animal welfare regulations.

Establishment of a mouse model of subacromial impingement and electroacupuncture treatment

Eighty 8-week-old male C57BL/6J mice were purchased to build subacromial impingement-induced chronic rotator cuff injury models per established protocols. Animals received general anesthesia, left shoulder incision and subacromial space implantation of a 2 mm titanium vascular clip, wounds were sutured and postoperative antibiotics were given for 3 days. A total of 80 healthy mice were ultimately selected for inclusion in the experimental study. This mouse model was designed to simulate the chronic tendon injury caused by subacromial mechanical impingement in humans. Four weeks after clip implantation, model construction was completed (Mod group). After clip removal, mice receiving electroacupuncture treatment for 2 or 4 weeks were assigned to the Mod+EA2W and Mod+EA4W groups, respectively. Following clip removal, additional mice were subjected to the same experimental conditions as the EA-treated groups— including daily anesthesia and identical handling procedures but without electroacupuncture intervention. These mice were defined as the Mod+2W and Mod+4W groups *(Fig. S1)*.

Electroacupuncture was applied at the left "Jianyu (LI15)" and "Jianliao (SJ14)" acupoints using sterile needles (0.16 mm diameter, 13 mm length) inserted to a depth of 4 mm beneath the skin. A dense disperse alternating waveform with a pulse width of 0.2 ms was delivered, and real time impedance monitoring was performed throughout stimulation, maintaining impedance within 1–5 kΩ. Electrical parameters were set at 2 Hz and 0.1 mA

© 2026 The Author(s) - Doi: 10.32098/mltj_2026_7232

for 15 min daily using a HANS apparatus. All mice in both experimental and control groups were anesthetized with isoflurane (1.5%, 500 ml/min) during treatment to ensure a stable deep anesthesia state. EA intervention began 24 h after removal of the vascular clip. No adverse events—including bleeding, local swelling, limping, or mortality—were observed in any animals during the treatment period.

Behavioral Analysis in Mice

Open field test (OFT)

10 mice from each group were selected for OFT behavioral assessment. Mice were placed individually in a 50 × 50 × 40 cm open field for free movement lasting 10 min. Total moving distance was recorded by overhead camera and quantified with EthoVision 14.0 software.

Footprint analysis (FA)

10 mice from each group were selected for FA. Forepaws were stained with blue pigment; mice walked uniformly on blank paper, and scanned footprints were used for subsequent data analysis.

Accelerating rotarod test (ART)

10 mice from each group were selected for the ART. Mice underwent balance assessment on a 3 cm-diameter rotating rod accelerating from 4 to 40 rpm within 5 min, with fall-off latency recorded. Each mouse completed three separated trials (15 min rest between trials), and average latency was adopted for statistics.

Biomechanical assessment of the rotator cuff

Grip strength test (GST)

10 mice from each group were selected for the GST. Grip strength was detected one day before specimen collection. Mice gripped the test bar with forelimbs at 45°, then pulled slowly until paw release to record peak tension. Three detections (≥30 min interval) per animal were averaged as final data.

Biomechanical testing (BT)

For biomechanical testing, 5 mice were randomly selected from each experimental group. Prior to mechanical loading, the mid substance width and thickness of the supraspinatus tendon were measured under a stereomicroscope using a digital micrometer. The cross sectional area was calculated using a rectangular approximation (width × thickness), and all measurements were recorded for subsequent stress normalization. Rotator cuff tendon-humerus complexes were fixed on Instron 5942 equipment for tensile biomechanical detection. After 0.1 N preloading, samples were stretched at 0.1 mm/s until rupture; specimens with tendon slipping or abnormal fracture were discarded.

Measurement of supraspinatus muscle volume

Using the same five mice selected for BT, supraspinatus,muscles were isolated and immersed in calibrated 1 ml water-filled graduated cylinders. Displaced water volume was measured in triplicate, and averaged value represented muscle volume.

Histological analysis (HA)of rotator cuff repair in mice

5 mice were randomly selected from each experimental group. Tissue specimens were sliced into 4 μm sections and stained with H&E, Safranin O-Fast Green and toluidine blue following our previously reported protocol[17]. Two independent researchers (ZC and ZWu) selected observation fields under a 10× lens; disputes were settled by a third assessor. Tendon-bone repair quality was scored with the modified Bonar system[18] *(Table 1)* based on tendon structural indexes. All histological slides were anonymized by a third researcher, who randomized the order and assigned new numerical codes to conceal group information. The two independent evaluators performed histological scoring in a fully blinded manner without any knowledge of experimental grouping.

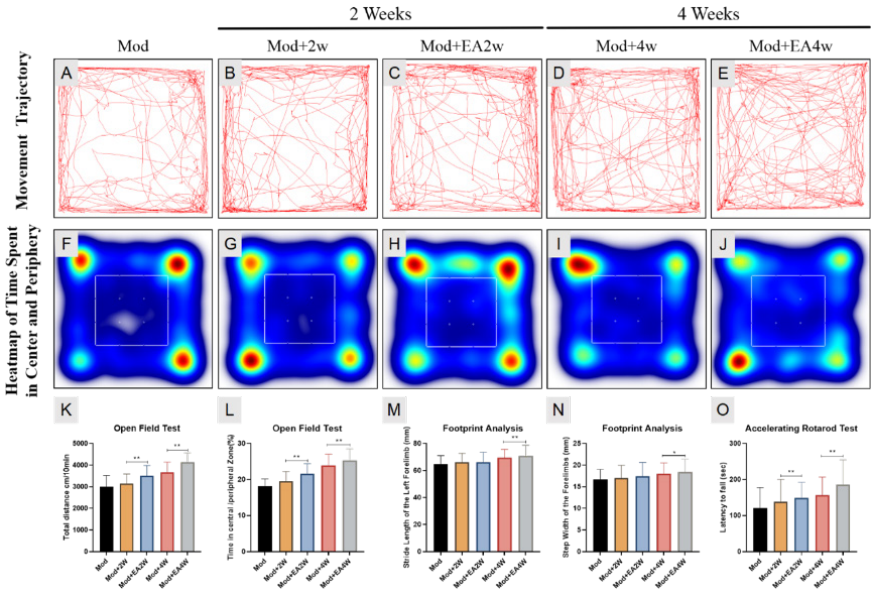


Figure 1. *(A-E) Trajectory diagrams of open-field spontaneous movement; (F-J) heatmap reflecting mice residence preference in central and peripheral regions. (K-O) Statistical plots of total moving distance, central occupation ratio, left forelimb step length, forelimb step width and rotarod falling latency, (n=10); *P<0.05, **P<0.01, ***P<0.001.*

© 2026 The Author(s) - Doi: 10.32098/mltj_2026_7232

Modified Bonar score for mouse rotator cuff tendon[18]				
	Grade 0	**Grade 1**	**Grade 2**	**Grade 3**
Cell morphology Three fields of view[a] H&E	Inconspicuous elongated spindle shaped nuclei with no obvious cytoplasm at light microscopy	Increased roundness: nucleus becomes more ovoid to round in shape without conspicuous cytoplasm	Increased roundness and size; the nucleus is round, slightly enlarged and a small amount of cytoplasm is visible	Nucleus is round, large with abundant cytoplasm and lacuna formation (chondroid change)
Cellularity Three fields of view H&E	Mainly discrete cells	Hypercellular[b]	Very hypercellular[c]	Areas of hyper[b] as well as hypo[d] cellularity with clear heterogeneity of cell distribution
Collagen derangement Polarized One field of view Picrosirius Red	Collagen arranged in tightly cohesive well demarcated bundles with a smooth dense bright homogenous polarization pattern with normal crimping	Diminished fiber polarization with maintenance of overall bundle architecture. Non-homogeneous polarization	Bundle changes; separation and loss of demarcation of fiber bundles, giving rise to expansion of the tissue overall and clear loss of normal polarization pattern	Marked separation of fiber bundles with complete loss of architecture
Vascularity ≤5 fields of view Vascular immunostain (Factor VIII)	Inconspicuous blood vessels coursing between bundles	Increased vascular immunostaining, occasional cluster of vessel, <2 per 5 fields of view	2–3 clusters of vessels per 5 fields of view	Areas with greater than 3 clusters per 5 fields of view, and/or areas of pathological avascularity
Ground substance One field of view Alcian Blue	Minimal ground substance	Stainable mucin with discrete bundles	Stainable mucin within bundles with loss of clear demarcation of bundles	Abundant mucin throughout the section with inconspicuous collagen staining

Table 1. *The histological evaluation score system.*

Legend: [a]Field of view: 100 x 100μm square; [b]Hypercellular: >50 nuclei per field; [c]Very hypercellular: >80 nuclei per field; [d]Hypocellular: <30 nuclei per field. IHC replaced Picrosirius Red for assessing collagen derangement; HE replaced Factor VIII to evaluate vascularity indicators.

Immunohistochemistry (IHC) test

Using the histological sections obtained from the five mice selected for HA analysis, immunohistochemical staining was performed to evaluate tendon-repair-related collagens in the rotator cuff according to previously reported procedures. Briefly, paraffin sections were deparaffinized and subjected to antigen retrieval, followed by overnight incubation at 4°C with the corresponding primary antibodies: COL1A1 (72026T, CST, USA), COL2A1 (600-401-104-05, Thermo Fisher, USA), and COL3A1 (22734-1-AP, Proteintech, USA). After three washes with PBS, the sections were incubated with biotin-labeled secondary antibodies: Goat Anti-Rabbit IgG HRP (ab6721, Abcam, UK). Visualization was achieved using DAB substrate (CST, 8509P, USA). All images were acquired with a light microscope (390335, Leica, Germany). Staining intensity within regions of interest (ROIs) was quantified using ImageJ. The staining intensity of the Mod group was used as the reference for normalization in subsequent statistical analyses.

Gene expression profiling of affected tendons following electroacupuncture treatment

6 mice from the Mod+2W and Mod+EA2W groups were euthanized after 2 weeks of electroacupuncture treatment, mice in the Mod+2W and Mod+EA2W groups were euthanized, and supraspinatus tendon specimens were harvested. Total RNA was isolated from cells using the TRIzol® Plus kit (Takara Technologies, D9108A, Shiga, Japan) previously reported methods[19].

First-strand cDNA synthesis was performed with the Synthesis SuperMix kit (TransGen, AQ211, China). Primer sequences used for amplification are listed in *Table 2*. Quantitative real-time PCR (qRT-PCR) was conducted with Fast SYBR® Green Master Mix (Life Technologies) in conjunction with a one-step real-time PCR kit (Applied Biosystems). Each qRT-PCR assay was repeated in triplicate across at least three independent experiments. Relative gene expression levels were calculated using the standard 2^(-ΔΔCt) method, with GAPDH serving as the internal control.

© 2026 The Author(s) - Doi: 10.32098/mltj_2026_7232

Western blot assay

9 mice from the Mod+2W and Mod+EA2W groups were selected. After 2 weeks of electroacupuncture treatment, mice in the Mod+2W and Mod+EA2W groups were sacrificed, and supraspinatus tendon specimens were collected. Western blotting was performed strictly according to previously reported standardized procedures[20].

After overnight incubation with primary antibodies at 4°C, the membranes were washed. The primary antibodies used included IL-1β (12242T, CST, USA), IL-6 (12912T, CST, USA), Tnf-α (11948T, CST, USA) Mmp-13 (67329T, CST, USA), Col1a1 (72026T, CST, USA), Col3a1 (ab184993, Abcam, UK), Scx (PA5-23943, Thermo Fisher, USA), Tnmd (ab203676, Abcam, UK) and Fabp4 (2120S, CST, USA). Subsequently, the membranes were incubated with the HRP-conjugated anti-rabbit IgG secondary antibody (CST, Cat. No. 7074, USA) at room temperature for 1 hour. Protein bands were visualized using Western ECL substrate (Bio-Rad, USA; Cat. No. 170-5061) and imaged with the Tanon 5200 enhanced chemiluminescence detection system (Tanon, China).

Statistical analysis

GraphPad Prism 8.0 and SPSS 20.0 were used for plotting and statistical calculation. Multiple-group comparison adopted one-way ANOVA with LSD post hoc test (Dunnett's test for unequal variance); two-group comparison used two-tailed Student's t-test. All data were expressed as mean ± SD, and p <0.05 meant statistical difference.

RESULTS

Electroacupuncture improves shoulder joint motor function in mice with chronic rotator cuff injury

Open-field test revealed motor function recovered in 2-week and 4-week groups compared with Mod group, accompanied by increased total movement distance and central zone exploration time *(Fig. 1A-E)*. Mod group had the minimum travel distance, implying impaired spontaneous activity after rotator cuff injury. Compared with non-acupuncture counterparts, EA increased total locomotor distance by 351 cm at 2 weeks (Mod+2W: 3149 ± 433 cm; Mod+EA2W: 3500 ± 482 cm), p = 0.002, and 471 cm at 4 weeks (Mod+4W: 3663 ± 474 cm; Mod+EA4W: 4134 ± 424 cm), p = 0.007 *(Fig. 1K)*. Central activity ratio was lowest in Mod (18.17% ± 1.99%). EA elevated central time proportion by 1.94% at 2 weeks (p = 0.009) and 1.34% at 4 weeks (p = 0.007), with statistical significance at both time points *(Fig. 1F-J and L)*. Footprint analysis indicated EA ameliorated forelimb gait performance. Left forelimb step length rose slightly after 2-week EA (Mod+2W: 65.94 ± 6.74 mm, Mod+EA2W: 66.13 ± 7.36 mm) and improved markedly at 4 weeks (Mod+4W: 69.54 ± 6.07 mm, Mod+EA4W: 71.02 ± 7.61 mm, p = 0.005, *Fig. 1M*). For step width, EA generated mild elevation at 2 weeks (Mod+2W:16.95 ± 2.98 mm, Mod+EA2W:17.43 ± 3.16 mm) and significant improvement at 4 weeks (Mod+4W:17.98 ± 2.54 mm, Mod+EA4W:18.36 ± 2.98 mm, p < 0.048, *Fig. 1N*). Consistent with above results, rotarod test validated improved coordination after EA. EA prolonged balance retention time by 10.16 s at 2 weeks (p

Gene name	Forward (5'→3')	Reverse (5'→3')
IL-1β	AGGAGAACCAAGCAACGACA	TGGGTGTGCCGTCTTTCATT
IL-6	GGAGCCCACCAAGAACGATAG	GTGAAGTAGGGAAGGCCGTG
IL-10	CTGCCGCTTTGCAGGTGTA	CATTGTGGGCAAGGTGCTATT
Tnf-α	GGTGCCTATGTCTCAGCCTCTT	GCCATAGAACTGATGAGAGGGAG
Mmp-13	TGGCTTAGAGGTGACTGGCA	CCACATCAGGCACTCCACAT
Col-1a1	GCTCGTGGAAATGATGGTGC	ACACCCTGGGGACCTTCAGA
Col-3a1	ACGTAAGCACTGGTGGACAG	CAGGAGGGCCATAGCTGAAC
Scx	GCTTTCTTCCACAGCGGTC	GTCACGGTCTTTGCTCAACTT
Tnmd	TGGGGGAGCAAACACTTCTG	TCGCCGTTGCTGTAGAAAGT
Ppary	CCAGAGCATGGTGCCTTCGCT	CAGCAACCATTGGGTCAGCTC
Fabp4	AAGGTGAAGAGCATCATAACCCT	TCACGCCTTTCATAACACATTCC
Sod2	CAGACCTGCCTTACGACTATGG	CTCGGTGGCGTTGAGATTGTT
Gpx1	CCACCGTGTATGCCTTCTCC	AGAGAGACGCGACATTCTCAAT
Gapdh	TGTGTCCGTCGTGGATCTGA	TTGCTGTTGAAGTCGCAGGAG

Table 2. *Primer sequences used for RT- PCR.*

© 2026 The Author(s) - Doi: 10.32098/mltj_2026_7232

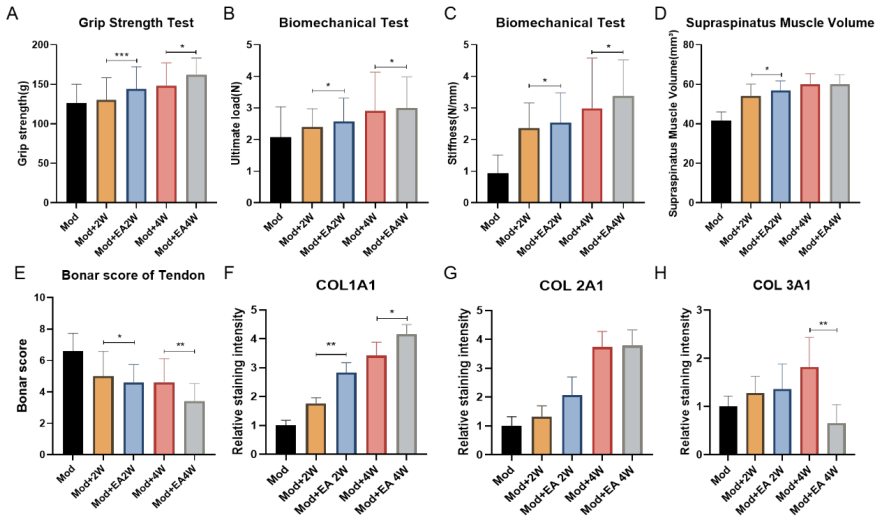


Figure 2. *A) Quantitative results of forelimb grip strength (n = 10); B, C) Tendon ultimate load and stiffness from biomechanical detection (n = 5); D) Supraspinatus muscle volume statistics (n = 5); E) Modified Bonar histological scoring data (n = 5); F-G) IHC staining for COL1A1, COL2A1 and COL3A1 protein relative staining intensity analysis (n = 5); *p <0.05, **p <0.01, ***p <0.001.*

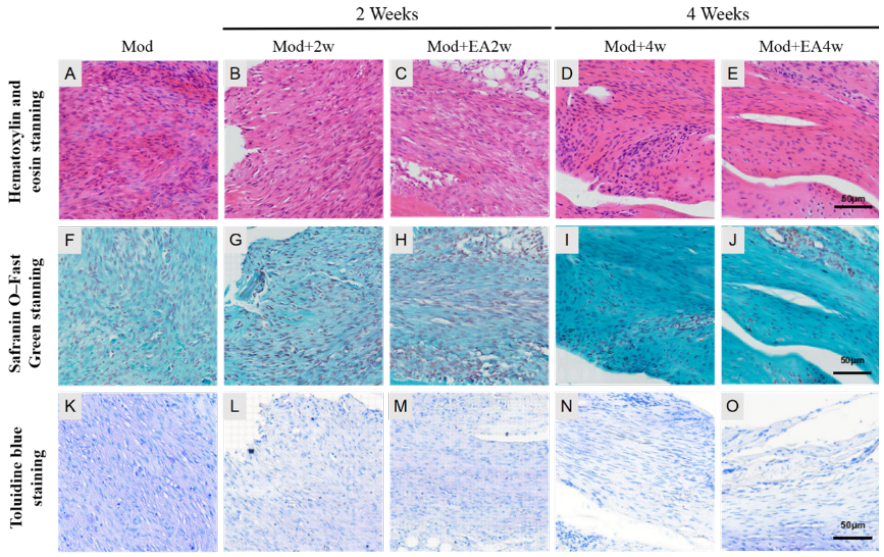


Figure 3. *Representative histological images of five experimental groups, including H&E (A-E), Safranin O-Fast Green (F-J) and Toluidine Blue (K-O) staining, (n = 5, scale bar 50 μm); *p <0.05, **p <0.01, ***p <0.001.*

= 0.018) and approximately 30 s at 4 weeks (p <0.001, *Fig. 1O*).

Electroacupuncture alleviates muscle atrophy and improves biomechanical properties of the shoulder joint in mice with chronic rotator cuff injury

Forelimb grip strength testing demonstrated EA effectively boosted forelimb grip strength of injured mice, with Mod group at 126.13 ± 23.85 g. Relative to untreated controls, EA raised grip strength by 14 g at 2 weeks (Mod+2W:130.49 ± 27.98 g; Mod+EA2W:144.30 ± 27.94 g) and 15 g at 4 weeks (Mod+4W:147.96 ± 29.29 g; Mod+EA4W:162.13 ± 21.20 g), all p <0.001 *(Fig. 2A)*. Biomechanical assays of supraspinatus tendon verified EA improved tendon mechanical properties. The ultimate load of Mod was 2.08 ± 0.96 N; EA elevated ultimate load at both time points (Mod+2W:2.39 ± 0.59 N, Mod+EA2W: 2.57 ± 0.74 N, p = 0.045; Mod+4W: 2.91 ± 1.22 N, Mod+EA4W: 3.00 ± 0.99 N, p = 0.012, *Fig. 2B*). For tendon stiffness (Mod: 0.94 ± 0.58 N/mm), stiffness values increased after EA intervention (Mod+2W: 2.36 ± 0.80 N/mm, Mod+EA2W: 2.54 ± 0.94 N/mm, p = 0.041; Mod+4W: 2.98 ± 1.60 N/mm, Mod+EA4W: 3.39 ± 1.14 N/mm, p = 0.032, *Fig. 2C*). Supraspinatus muscle volume was detected via water-displacement method[21]. Mod muscle volume was 41.74 ± 4.22 mm^3. EA significantly increased muscle volume at 2 weeks (Mod+2W: 53.98 ± 6.07 mm^3, Mod+EA2W: 56.90 ± 4.92 mm^3, p = 0.031), whereas no statistical difference existed at 4 weeks (Mod+4W: 59.89 ± 5.54 mm^3, Mod+EA4W: 60.00 ± 4.88 mm^3, p = 0.462, *Fig. 2D*), indicating EA mainly alleviated early muscle atrophy

Electroacupuncture enhances tendon fiber repair in the shoulder joint of mice with chronic rotator cuff injury

Histological observation was performed on rotator cuff tendon samples from all five experimental groups. H&E staining showed severe tendon damage in Mod group, including disordered collagen, fiber breakage and massive inflammatory infiltration *(Fig. 3A)*. Spontaneous recovery brought limited structural improvement in Mod+2W and Mod+4W, while EA treatment obviously alleviated pathological manifestations, especially in Mod+EA4W with neatly aligned mature collagen and decreased inflammation *(Fig. 3B-E)*. Quantitative Bonar

scores peaked at 6.60 ± 1.14 in Mod group; EA reduced scores to 4.60 ± 1.14 at 2 weeks (Mod+2W: 5.00 ± 1.58, p = 0.0026) and 3.40 ± 1.14 at 4 weeks (Mod+4W: 4.60 ± 1.52, p = 0.003, *Fig. 2E*). Safranin O-Fast Green staining displayed sparse collagen and faint green staining in Mod and Mod+2W *(Fig. 3F-G)*. Fiber arrangement was partially optimized in Mod+EA2W, and Mod+EA4W possessed compact, deep-green orderly collagen bundles *(Fig. 3H-J)*. Toluidine Blue staining presented scarce ECM and weak purple staining in Mod, Mod+2W and Mod+EA2W *(Fig. 3K-M)*. Mod+4W had scattered mild staining, whereas Mod+EA4W obtained intensive uniform staining, elevated glycosaminoglycan and abundant encapsulated ECM around tendon cells *(Fig. 3N-O)*. Collectively, EA facilitates ECM synthesis and collagen maturation to accelerate tendon structural repair.

Electroacupuncture enhances collagen protein expression in supraspinatus tendon fibers of mice with chronic rotator cuff injury

Immunohistochemical staining was performed to evaluate the expression levels of Collagen type I alpha 1 chain (COL1A1), Collagen type II alpha 1 chain (COL2A1), and Collagen type III alpha 1 chain (COL3A1) in injured tendon tissues. In the Mod and Mod+2W groups, COL1A1 staining showed weak positivity, with sparsely distributed chromogenic granules, limited positive areas, and disrupted, disorganized collagen fibers. The relative staining intensity in the Mod+2W group was 1.76±0.23 *(Fig. 2F and Fig. 4A–B)*. In contrast, the Mod+EA2W group exhibited improved staining, showing moderate positivity with a relative intensity of 2.83 ± 0.43. The positive staining area expanded within the central injury region, and collagen fiber alignment was visibly improved. A significant difference was observed between the 2-week subgroups (p = 0.001) *(Fig. 2F and Fig. 4C)*. At 4 weeks, the Mod+4W group displayed strong COL1A1 staining (3.42 ± 0.58), although tendon cells remained immature. The Mod+EA4W group showed the strongest and most widespread positive staining (4.15 ± 0.45), with collagen fibers arranged in parallel and orderly patterns, resembling near-normal tendon morphology. The difference between the 4-week subgroups was statistically significant (p = 0.024) *(Fig. 2F and Fig. 4D–E)*. The Mod and Mod+2W groups exhibited extremely weak COL2A1 staining, with the Mod+2W group showing a relative intensity of 1.32 ± 0.45.

Positive signals were only sporadically distributed along the tendon margins *(Fig. 2F and Fig. 4F–G)*. In the Mod+EA2W group, a faint band like positive signal appeared in the tendon fusion zone, with increased expression and an expanded positive area (relative intensity: 2.07 ± 0.77) *(Fig. 2F and Fig. 4H)*. At 4 weeks, both the Mod+4W and Mod+EA4W groups demonstrated continuous moderate positivity, with relative intensities of 3.73 ± 0.66 and 3.78 ± 0.72, respectively. However, tendon cells remained immature in both groups *(Fig. 2F and Fig. 4I–J)*.

In the Mod and Mod+2W groups, moderate COL3A1 staining was observed only in granulation tissue at the tendon margins, whereas staining in the central injury region was weak, with disorganized collagen fibers. The relative intensity in the Mod+2W group was 1.28 ± 0.39 *(Fig. 2G and Fig. 4K–L)*. In the Mod+EA2W group, moderate positivity was present throughout the entire injury region, with increased positive area and initial formation of directionally aligned collagen fibers (relative intensity: 1.36 ± 0.65) *(Fig. 2G and Fig. 4M)*. The Mod+4W group maintained moderate positivity, but tendon cells remained irregular and immature, with disorganized collagen fiber arrangement (relative intensity: 1.82 ± 0.70) *(Fig. 2G and Fig. 4N)*. Notably, in the Mod+EA4W group, only weak COL3A1 staining was observed at the tendon margins, with a markedly reduced positive area (relative intensity: 0.65 ± 0.41). Collagen fibers were arranged in parallel and highly organized patterns, indicating substantially improved tendon repair quality. A significant difference was observed between the 4-week subgroups (p = 0.006) *(Fig. 2G and Fig. 4O)*.

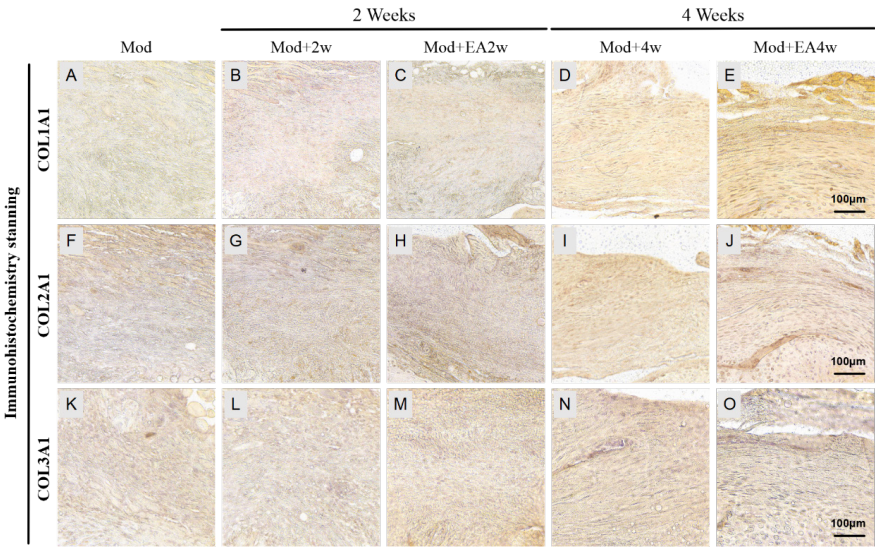


Figure 4. *IHC staining photographs for COL1A1 (A-E), COL2A1 (F-J) and COL3A1 (K-O) in supraspinatus tendon of each group, (n = 5, scale bar 100 μm).*

© 2026 The Author(s) - Doi: 10.32098/mltj_2026_7232

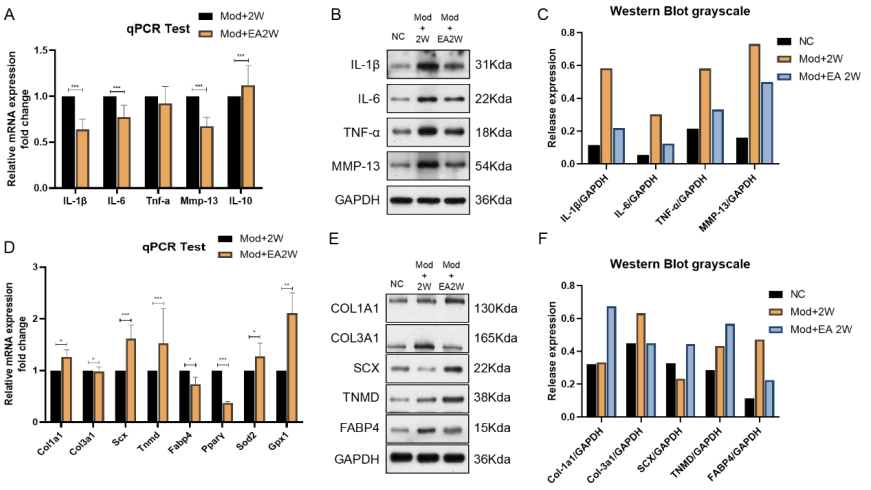


Figure 5. *mRNA and protein expression comparison between Mod+2W and Mod+EA2W groups, n = 3; A, D) qPCR results of inflammation-, tendon repair-, fat infiltration- and antioxidant-related genes, n = 3; B, E) corresponding Western blot band quantification, GAPDH served as internal reference; C, F) Quantification of expression levels based on grayscale values in Western blot (*p <0.05, **p <0.01, ***p <0.001).*

Electroacupuncture regulates the expression of different types of genes and proteins in supraspinatus tendon of mice with chronic rotator cuff injury

qPCR and Western blot were performed to detect molecular expression differences between Mod+2W and Mod+EA2W after two weeks of EA intervention. For inflammation-associated genes, EA reduced the expression of pro-inflammatory *Il-1β* by 0.638 ± 0.113 fold and *Il-6* by 0.772 ± 0.129 fold (both p <0.001), while *Tnf-α* presented a declining tendency without statistical significance(p = 0.472). Meanwhile, anti-inflammatory *Il-10* was upregulated by 1.121 ± 0.215 fold, and degradation-related *Mmp-13* was downregulated by 0.674 ± 0.099 fold (both p <0.001, *Fig. 5A*). Western blot results were consistent with mRNA data, with obvious declines of *Il-1β*, *Il-6* and *Mmp-13* protein in EA group *(Fig. 5B-C)*, proving EA relieves inflammatory response and tendon matrix degradation. For tendon structural and adipogenic genes, EA markedly elevated *Col1a1* by 1.26 ± 0.14 fold (p = 0.012), and maturation-related *Scx* and *Tnmd* by 1.62 ± 0.26 fold and 1.53 ± 0.67 fold respectively (both p <0.001); Scar-related *Col3a1* was downregulated by 0.58 ± 0.09 fold (p = 0.664). Besides, fatty infiltration-related *Pparγ* and *Fabp4* were separately decreased by 0.51 ± 1.03 fold and 0.85 ± 0.96 fold (both p <0.001). Antioxidant *Sod2* and *Gpx1* were upregulated by 1.27 ± 0.26 fold (p = 0.029) and 2.11 ± 0.39 fold (p = 0.030) after EA *(Fig. 5D)*. At protein level, *Col1a1*, *Scx* and *Tnmd* were upregulated, whereas *Col3a1* and adipogenic *Fabp4* were suppressed in Mod+EA2W *(Fig. 5E-F)*. Collectively, EA facilitates tendon maturation, inhibits fatty infiltration and alleviates oxidative injury to accelerate tendon repair.

DISCUSSION

Acupuncture has been applied in East Asia for over 6000 years[22], and WHO recommends acupuncture therapy for 77 types of illnesses[23]. Combining traditional acupuncture and modern electrotherapy, EA features convenient operation and negligible drug-related side effects and has been widely used for gout, neurogenic disorders and sports injury rehabilitation[24-26]. Nevertheless, conflicting clinical results emerge, such as one report denying additional therapeutic effects of EA for subacromial pain syndrome[27,28], which highlights the necessity of fundamental animal experiments to supplement clinical evidence; the present study therefore establishes an impingement-induced mouse rotator cuff injury model to clarify EA's repairing efficacy and provide experimental references for clinical application and reflections.

Open-field test is a classic method to evaluate spontaneous activity and anxiety state of injured rodents by measuring movement distance and central region residence ratio[29]. Our results confirmed EA for 2 and 4 weeks significantly increased total movement distance and central staying time, manifesting improved locomotor ability and alleviated anxiety; the anxiolytic effect of EA may stem from direct neural circuit regulation or indirect pain relief[23,30], yet the exact pathway remains unclear. Footprint and rotarod tests reflected limb gait and coordination: 2-week EA exerted limited gait improvement, while 4-week EA obviously increased forelimb step length and width; EA prolonged falling latency at both treatment durations, consistent with published clinical data showing electrical stimulation improves postoperative shoulder function in rotator cuff tear and arthroplasty patients[31,32]. Although EA treatment produced measurable improvements in functional performance and biomechanical strength, the early therapeutic effects were relatively modest. Moreover, the differences between groups became less pronounced at later observation time points. These findings suggest that the beneficial window of EA may extend beyond the current experimental duration. Future studies with longer follow up periods and optimized group allocation will be required to more precisely define the therapeutic boundaries and long term efficacy of EA.

Chronic rotator cuff injury commonly induces muscle atrophy, fatty infiltration and fibrosis to hinder tendon healing[33]. Previous literature has validated EA relieves skeletal muscle atrophy through IGF 1/PI3K/Akt or other pathways[34,35]. Our supraspinatus muscle volume data showed prominent anti-atrophy effect at 2 weeks, with no

© 2026 The Author(s) - Doi: 10.32098/mltj_2026_7232

statistical difference at 4 weeks; EA significantly raised forelimb grip strength at two time points via mitigating atrophy and pain[36]. Biomechanical indicators including tendon ultimate load and stiffness are gold standard for tendon functional evaluation[37], and combined with lower Bonar score[18] in EA-treated group, our data proved EA optimizes tendon mechanical property and histological maturity. Postoperative rotator cuff repair mostly generates scar tissue rich in COL3A1 instead of normal enthesis, leading to extremely high tendon re-tear rate up to 94%[38,39]. Healthy tendon relies on high-content regularly arranged COL1A1 (~90%) for mechanical stability, and elevated COL3A1 implies excessive scarring[40,41]. IHC demonstrated EA upregulated COL1A1 and COL2A1 expression without increasing COL3A1, elevating COL1A1/COL3A1 ratio to restrict scar hyperplasia and facilitate physiological tendon maturation. It is noteworthy that the biological implications of COL2A1 are dual in nature. Physiological fibrocartilage formation is characterized by orderly collagen II and proteoglycan deposition, which supports favorable tendon–bone integration. In contrast, excessive or disorganized accumulation reflects pathological chondrogenic metaplasia, a hallmark of tendon degeneration and impaired healing. In our study, EA treatment did not produce significant differences in COL2A1 expression among the experimental groups, suggesting that EA may not substantially influence the fibrocartilage-related component of tendon remodeling under the current experimental conditions.

Multiple molecular pathways participate in EA-mediated tendon repair: excessive oxidative stress damages tendon construction, and EA upregulates antioxidant *Sod2* and *Gpx1* to resist ROS injury[42,43], pro-inflammatory *Il 1β* suppresses collagen synthesis and tendon marker expression while inducing *Mmp13* to aggravate tendon degradation[44,45]. In patients with tendinopathy and rotator cuff disease, pro-inflammatory macrophages in tendon tissue are usually positively correlated with disease severity[46], and our study shows that EA effectively reduces the levels of such inflammatory factors. The *Pparγ-Fabp4* axis dominates tendon fatty infiltration[47,48], and *Fabp4* can further activate inflammatory cytokines to worsen tendon lesion[49], our findings confirm EA inhibits *Pparγ* and *Fabp4* expression to reduce adipocyte deposition, serving as a core therapeutic mechanism requiring deeper mechanistic exploration. In addition, it remains debatable whether tendon structural restoration necessarily translates to improved muscle strength and functional recovery, as many clinical patients with degenerative rotator cuff tears still maintain relatively satisfactory limb function. However, our study has several evident limitations. First, the behavioral assessments used including open field testing, footprint analysis, rotarod testing, and grip strength measurement can only indirectly reflect the recovery of shoulder function rather than directly representing it. In addition, human chronic rotator cuff disease is multifactorial, involving age related tendon degeneration, mechanical overload, metabolic disorders, vascular changes, fatty infiltration, scapular biomechanical alterations, and pain related dysfunction. The mouse model used in this study cannot fully recapitulate the clinical phenotype of human chronic rotator cuff pathology. Moreover, due to the limited availability of experimental specimens, our investigation focused only on the early molecular changes following electroacupuncture treatment (2 weeks). The effects at 4 weeks and longer term outcomes remain to be elucidated in future studies. Therefore, the translatability of findings from preclinical animal studies to human tendon injury treatment requires further investigation and validation.

CONCLUSION

In this mechanically induced rotator cuff injury model, low intensity electroacupuncture was associated with improvements in histological organization, biomechanical strength, inflammatory modulation, reduction of fatty infiltration markers, and enhancement of tendon maturation markers. However, before considering clinical translation, additional rigorously controlled preclinical studies including sham stimulation controls and extended follow up periods are required to more clearly define the therapeutic boundaries and long term benefits of EA.

REFERENCES

1. Meislin RJ, Sperling JW, Stitik TP. Persistent shoulder pain: epidemiology, pathophysiology, and diagnosis. American journal of orthopedics (Belle Mead, NJ). 2005;34(12 Suppl):5-9.
2. Mazzocca AD, Arciero RA, Shea KP, Apostolakos JM, Solovyova O, Gomlinski G, et al. The Effect of Early Range of Motion on Quality of Life, Clinical Outcome, and Repair Integrity After Arthroscopic Rotator Cuff Repair. Arthroscopy. 2017;33(6):1138-1148. doi: 10.1016/j.arthro.2016.10.017.
3. Jäschke M, Köhler HC, Weber MA, Tischer T, Hacke C, Schulze C. Subacromial impingement syndrome: association of multiple magnetic resonance imaging parameters with shoulder function and pain. Arch Orthop Trauma Surg. 2023;143(1):237-246. doi: 10.1007/s00402-021-04032-6.
4. Giri A, O'Hanlon D, Jain NB. Risk factors for rotator cuff disease: A systematic review and meta-analysis of diabetes, hypertension, and hyperlipidemia. Ann Phys Rehabil Med. 2023;66(1):101631. doi: 10.1016/j.rehab.2022.101631.
5. Chen Z, Jin M, He H, Dong J, Li J, Nie J, et al. Mesenchymal stem cells and macrophages and their interactions in tendon-bone healing. J Orthop Translat. 2023;39:63-73. doi: 10.1016/j.jot.2022.12.005.
6. Liu L, Yang F, Liao Y, Deng H, Le D, Zhang C, et al. Exploration of causal relationship between shoulder impingement syndrome and rotator cuff injury: a bidirectional mendelian randomization. BMC Musculoskelet Disord. 2024;25(1):649. doi: 10.1186/s12891-024-07556-1.
7. Yang J, Xiang M, Li Y, Zhang Q, Dai F. The Correlation between Various Shoulder Anatomical Indices on X-Ray and Subacromial Impingement and Morphology of Rotator Cuff Tears. Orthop Surg. 2023;15(8):1997-2006. doi: 10.1111/os.13610.
8. Prill R, Ma CB, Wong SE, Beaufils P, Monllau JC, Arhos EK, et al. The formal EU-US Meniscus Rehabilitation 2024 Consensus: An ESSKA-AOSSM-AASPT initiative. Part II-Prevention, non-operative treatment and return to sport. Knee Surg Sports Traumatol Arthrosc. 2025;33(8):3014-3024. doi: 10.1002/ksa.12689.
9. Ardern CL, Büttner F, Andrade R, Weir A, Ashe MC, Holden S, et al. Implementing the 27 PRISMA 2020 Statement items for systematic reviews in the sport and exercise medicine, musculoskeletal rehabilitation and sports science fields: the PERSiST (implementing Prisma in Exercise, Rehabilitation, Sport medicine and SporTs science) guidance. Br J Sports Med. 2022;56(4):175-195. doi: 10.1136/

© 2026 The Author(s) - Doi: 10.32098/mltj_2026_7232

bjsports-2021-103987.
10. Gottlieb U, Hayek R, Hoffman JR, Springer S. Exercise combined with electrical stimulation for the treatment of chronic ankle instability - A randomized controlled trial. J Electromyogr Kinesiol. 2024;74:102856. doi: 10.1016/j.jelekin.2023.102856.
11. Chang CY, Weng YH, Chang CH, Yang JL, Chen PT, Lin JJ. Neuromuscular electrical stimulation of humeral adductors in subjects with rotator cuff tear. Arch Orthop Trauma Surg. 2024;144(5):2039-2046. doi: 10.1007/s00402-024-05316-3.
12. Wang RS, Sun JN, Zheng QY, Chen L, Chen P. Therapeutic efficacy of home-based neuromuscular electrical stimulation on early postoperative functional recovery following arthroscopic rotator cuff repair: a double-blind randomized controlled trial. BMC Musculoskelet Disord. 2025;26(1):805. doi: 10.1186/s12891-025-09030-y.
13. Stewman CG. Ultrasound-Guided Electroacupuncture Treatment for Rotator Cuff Tendinopathy: Proposing an Effective Alternative to Nonoperative Medical Treatments. Med Acupunct. 2023;35(5):257-261. doi: 10.1089/acu.2023.0042.
14. Inoue M, Nakajima M, Oi Y, Hojo T, Itoi M, Kitakoji H. The effect of electroacupuncture on tendon repair in a rat Achilles tendon rupture model. Acupunct Med. 2015;33(1):58-64. doi: 10.1136/acupmed-2014-010611.
15. Imaeda M, Hojo T, Kitakoji H, Tanaka K, Itoi M, Inoue M. Effect of electroacupuncture stimulation on long-term recovery following Achilles tendon rupture in a rat model. Acupunct Med. 2018;36(5):327-332. doi: 10.1136/acupmed-2016-011292.
16. de Almeida Mdos S, de Aro AA, Guerra Fda R, Vieira CP, de Campos Vidal B, Rosa Pimentel E. Electroacupuncture increases the concentration and organization of collagen in a tendon healing model in rats. Connect Tissue Res. 2012;53(6):542-7. doi: 10.3109/03008207.2012.710671.
17. Chen Z, Liu Y, Liang T, Du Z, Deng L, Wu Z, et al. Enhanced rotator cuff tendon-bone interface regeneration with injectable manganese-based mesoporous silica nanoparticle-loaded dual crosslinked hydrogels. Front Bioeng Biotechnol. 2025;13:1645970. doi: 10.3389/fbioe.2025.1645970.
18. Fearon A, Dahlstrom JE, Twin J, Cook J, Scott A. The Bonar score revisited: region of evaluation significantly influences the standardized assessment of tendon degeneration. J Sci Med Sport. 2014;17(4):346-50. doi: 10.1016/j.jsams.2013.07.008.
19. Peng R, Yu B, Zhang L, Xue Z, Yao L, Yang Q, et al. Targeted Inhibition of CD74+ Macrophages by Luteolin via CEBPB/P65 Signaling Ameliorates Osteoarthritis Progression. Adv Sci (Weinh). 2026;13(7):e08472. doi: 10.1002/advs.202508472.
20. Chen Z, Wang X, Wang S, Wu Z, Wang H, Chiu K, et al. Lycium barbarum glycopeptide protects neurons from amyloid-beta toxicity. Neural Regen Res. 2026;21(10):5013-5019. doi: 10.4103/NRR.NRR-D-25-00501.
21. Brock Symons T, Park J, Kim JH, Kwon EH, Delacruz J, Lee J, et al. Attenuation of skeletal muscle atrophy via acupuncture, electro-acupuncture, and electrical stimulation. Integr Med Res. 2023;12(2):100949. doi: 10.1016/j.imr.2023.100949.
22. Wang SM, Kain ZN, White P. Acupuncture analgesia: I. The scientific basis. Anesth Analg. 2008;106(2):602-10. doi: 10.1213/01.ane.0000277493.42335.7b.
23. Zhang Q, Zhou M, Huo M, Si Y, Zhang Y, Fang Y, et al. Mechanisms of acupuncture-electroacupuncture on inflammatory pain. Mol Pain. 2023;19:17448069231202882. doi: 10.1177/17448069231202882.
24. Ni Z, Xiao Q, Xia Z, Kuang K, Yin B, Peng D. Electroacupuncture for acute gouty arthritis: a systematic review and meta-analysis of randomized controlled trials. Front Immunol. 2024;14:1295154. doi: 10.3389/fimmu.2023.1295154.
25. Han Q, Chen P, Chen X, Wang L, Huang R, Li W, et al. The Neuroprotective Effects of Electroacupuncture on Parkinson's Disease and the Underlying Molecular Mechanisms. J Integr Neurosci. 2024;23(1):11. doi: 10.31083/j.jin2301011.
26. Li WX, Wu CQ, Feng W, Zhan YJ, Yang L, Jia HJ, et al. Acupuncture for rehabilitation after total knee arthroplasty: a systematic review and network meta-analysis. Int J Surg. 2025;111(1):1373-1385. doi: 10.1097/JS9.0000000000002006.
27. Lewis J, Sim J, Barlas P. Acupuncture and electro-acupuncture for people diagnosed with subacromial pain syndrome: A multicentre randomized trial. Eur J Pain. 2017;21(6):1007-1019. doi: 10.1002/ejp.1001.
28. Wu JJ, Weis MA, Kim LS, Eyre DR. Type III collagen, a fibril network modifier in articular cartilage. J Biol Chem. 2010;285(24):18537-44. doi: 10.1074/jbc.M110.112904.
29. Zhao Z, Wu X, Wu W, Tang Y, Meng X, Peng M, et al. The Potential Related Genes and Mechanisms Involved in Improving the Treadmill Exercise Ability of APP/PS1 Mice. Int J Mol Sci. 2024;25(19):10244. doi: 10.3390/ijms251910244.
30. Wu Z, Shen Z, Xu Y, Chen S, Xiao S, Ye J, et al. A neural circuit associated with anxiety-like behaviors induced by chronic inflammatory pain and the anxiolytic effects of electroacupuncture. CNS Neurosci Ther. 2024;30(4):e14520. doi: 10.1111/cns.14520.
31. Weng YH, Wong CK, Chien YT, Yang JL, Chang CH, Lin JJ. Novel brace with long-duration neuromuscular electrical stimulation in patients with full-thickness rotator cuff tears: A randomized controlled trial. Clin Rehabil. 2025;39(9):1197-1208. doi: 10.1177/02692155251356455.
32. Lee JH, Chun YM, Kim DS, Lee DH, Shin SJ. Effects of neuromuscular electrical muscle stimulation on the deltoid for shoulder function restoration after reverse total shoulder arthroplasty in the early recovery period: a prospective randomized study. Arch Orthop Trauma Surg. 2023;143(6):3037-3046. doi: 10.1007/s00402-022-04515-0.
33. Papadopoulos P, Wang C, Savoie FH, 3rd, You Z, Ge D. Oxandrolone treatment prevents muscle atrophy and retraction after rotator cuff injury: an experimental study in rats. JSES Rev Rep Tech. 2025;5(4):625-634. doi: 10.1016/j.xrrt.2025.08.003.
34. Huang XQ, Xu JS, Ye XR, Chen X. Wide Pulse Width Electroacupuncture Ameliorates Denervation-Induced Skeletal Muscle Atrophy in Rats via IGF-1/PI3K/Akt Pathway. Chin J Integr Med. 2021;27(6):446-454. doi: 10.1007/s11655-021-2865-0.
35. Su Z, Robinson A, Hu L, Klein JD, Hassounah F, Li M, et al. Acupuncture plus Low-Frequency Electrical Stimulation (Acu-LFES) Attenuates Diabetic Myopathy by Enhancing Muscle Regeneration. PLoS One. 2015;10(7):e0134511. doi: 10.1371/journal.pone.0134511.
36. Shah S, Godhardt L, Spofford C. Acupuncture and Postoperative Pain Reduction. Curr Pain Headache Rep. 2022;26(6):453-458. doi: 10.1007/s11916-022-01048-4.
37. Yonemitsu R, Tokunaga T, Shukunami C, Ideo K, Arimura H, Karasugi T, et al. Fibroblast Growth Factor 2 Enhances Tendon-to-Bone Healing in a Rat Rotator Cuff Repair of Chronic Tears. Am J Sports Med. 2019;47(7):1701-1712. doi: 10.1177/0363546519836959.
38. Vervaecke AJ, Carbone AD, Abraham A, Bernstein Z, Laudier D, Verborgt O, et al. Tendon progenitor cells as biological augmentation improve functional gait and reduce scar formation after rotator cuff repair. J Shoulder Elbow Surg. 2022;31(11):2366-2380. doi: 10.1016/j.jse.2022.05.004.
39. Zhao J, Luo M, Pan J, Liang G, Feng W, Zeng L, et al. Risk factors affecting rotator cuff retear after arthroscopic repair: a meta-analysis and systematic review. J Shoulder Elbow Surg. 2021;30(11):2660-2670. doi: 10.1016/j.jse.2021.05.010.
40. Thankam FG, Dilisio MF, Gross RM, Agrawal DK. Collagen I: a kingpin for rotator cuff tendon pathology. Am J Transl Res. 2018;10(11):3291-3309.
41. Paping A, Basler C, Ehrlich L, Fasting C, Melchior K, Ziska T, et al. Uterine scars after caesarean delivery: From histology to the molecular and ultrastructural level. Wound Repair Regen. 2023;31(6):752-763. doi: 10.1111/wrr.13127.
42. Yamaura K, Mifune Y, Inui A, Nishimoto H, Kurosawa T, Mukohara S, et al. Antioxidant effect of nicotinamide mononucleotide in tendinopathy. BMC Musculoskelet Disord. 2022;23(1):249. doi: 10.1186/s12891-022-05205-z. Erratum in: BMC Musculoskelet Disord. 2022 Jun 6;23(1):541. doi: 10.1186/s12891-022-05424-4.
43. Morikawa D, Nojiri H, Itoigawa Y, Ozawa Y, Kaneko K, Shimizu T. Antioxidant treatment with vitamin C attenuated rotator cuff degeneration caused by oxidative stress in Sod1-deficient mice. JSES Open Access. 2018;2(1):91-96. doi: 10.1016/j.jses.2017.11.003.
44. Zhang K, Asai S, Yu B, Enomoto-Iwamoto M. IL-1β irreversibly inhibits tenogenic differentiation and alters metabolism in injured tendon-derived progenitor cells in vitro. Biochem Biophys Res Commun. 2015;463(4):667-72. doi: 10.1016/j.bbrc.2015.05.122.
45. Sun HB, Li Y, Fung DT, Majeska RJ, Schaffler MB, Flatow EL. Coordinate regulation of IL-1beta and MMP-13 in rat tendons following subrupture fatigue damage. Clin Orthop Relat Res. 2008;466(7):1555-61. doi: 10.1007/s11999-008-0278-4.
46. Ackerman JE, Best KT, Muscat SN, Loiselle AE. Metabolic Regulation of Tendon Inflammation and Healing Following Injury. Curr Rheumatol Rep. 2021;23(3):15. doi: 10.1007/s11926-021-00981-4.
47. Lin D, Alberton P, Caceres MD, Volkmer E, Schieker M, Docheva D. Tenomodulin is essential for prevention of adipocyte accumulation and fibrovascular scar formation during early tendon healing. Cell Death Dis. 2017;8(10):e3116. doi: 10.1038/cddis.2017.510.
48. Park SJ, Lee YS, Yoon JP, Chung SW. Fenofibrate Attenuates Rotator Cuff Muscle Fatty Infiltration via Modulation of the PPARα-FABP4 Pathway. Am J Sports Med. 2025;53(14):3474-3482. doi: 10.1177/03635465251382858.
49. Ma Z, Lee AYW, Kot CH, Yung PSH, Chen SC, Lui PPY. Upregulation of FABP4 induced inflammation in the pathogenesis of chronic tendinopathy. J Orthop Translat. 2024;47:105-115. doi: 10.1016/j.jot.2024.06.007.

SUPPLEMENTARY MATERIALS

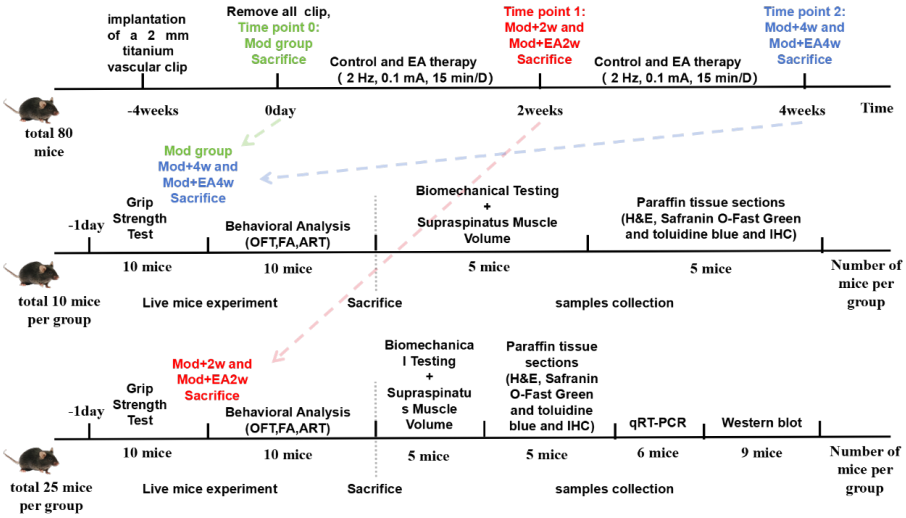


Figure S1. *Animal flow diagram of animal modelling for mouse rotator cuff injury induced by subacromial impingement treated with Low Intensity Electroacupuncture.*

© 2026 The Author(s) - Doi: 10.32098/mltj_2026_7232